TRANSITUS

Received
May 20, 2025

Revised
July 12, 2025

Accepted
August 10, 2025

Published
September 13, 2025

Keywords
Dispersive Solitons; Cole-Hopf transformation; Direct symbolic approach; Bilinear form; Wave interactions.

Higher-order rogue waves and their interactions to a generalized Kadomtsev–Petviashvili influenced evolution equation in fluid dynamics

Brij Mohan[†], Raj Kumar[‡], Virendra Kumar[§]

[†]Department of Mathematics, Hanraj College, University of Delhi, Delhi -110007, India

[‡]Department of Mathematics, Kirori Mal College, University of Delhi, Delhi 110007, India

[§]Department of Mathematics, Daulat Ram College, University of Delhi, Delhi -110007, India

Corresponding Author: V. Kumar (vmath.du@gmail.com)

DOI/url: https://journalmanager.transitus.in/index.php/jamss

Abstract: This paper investigates rogue waves in the (3+1)-dimensional potential Kadomtsev–Petviashvili equation, with a specific focus on the B-type Kadomtsev–Petviashvili equation in fluid dynamics. It employs a direct symbolic approach with a generalized formula to generate higher-order rogue waves with arbitrary parameters. The study establishes the Hirota D-operator bilinear form of the equation under investigation. The research produces two- and three-rogue wave interactions for the second-order and third-order rogue solutions, illustrating that significant rogue waves interact locally within nonlinear processes. A bilinear equation is derived using a dependent variable transformation, with ξ and η serving as the transforming variables. The analysis of the dynamical behavior showcases the exact solutions derived in the new variables ξ and η, as well as the initial variables x, y, z, and t, utilizing the symbolic system Mathematica. The study highlights the importance of larger waves with smaller amplitudes and their evolution in fluid dynamics, water engineering, and dispersive media. This equation provides insights into these phenomena. Rogue waves have implications across various scientific fields, including dusty plasma, oceanography, plasma physics, optical fibers, and other nonlinear systems.

1 Introduction

The potential Kadomtsev–Petviashvili (pKP) equation with the B-type Kadomtsev–Petviashvili equation (pKP-BKP) constructs a type of integrable system within the broader KP hierarchy. It combines the potential Kadomtsev-Petviashvili (pKP) [1–3] and B-type Kadomtsev-Petviashvili (BKP) [4–6] equations, and finds applications in fluid dynamics, oceanography, plasma physics, water engineering, optical fibers, and nonlinear systems. This equation is useful in modeling wave interactions and incorporating properties from both the pKP and BKP equations. Its solutions are a fascinating area of study with their complex and rich nature. And, offers a valuable tool for understanding and predicting nonlinear wave phenomena. The well-known KP equation [7, 8] is a nonlinear partial differential equation (PDE) that generalizes the Korteweg-de Vries (KdV) equation [9,10] to two spatial dimensions. The BKP equation is a variantion of the KP equation that deals with a bosonic fields in KP hierarchy. It focuses on different symmetry properties and constraints. The pKP-BKP equation, on the other hand, is a combination of these equations that incorporates their unique properties and constraints. It is beneficial in situations with positive and negative waves, such as studying wave interactions in plasma physics.
The specific form of the pKP-BKP equation can vary, but it typically includes terms that reflect the system's integrable nature and the interactions between the involved waves. Research on the pKP-BKP equation is a dynamic and ongoing process, constantly striving to find exact solutions, study the integrability properties, and explore the rich structure of these solutions, including solitons, lump solutions, and other localized waveforms. This continuous exploration keeps the field of fluid dynamics, water engineering, plasma physics, and optical fibers vibrant and exciting, offering new insights and applications.
This study investigates higher-order rogue waves for the pKP-BKP equation [11] in fluid dynamics as

$$u_{xt}+\alpha\left(45u_x^2u_{xx}+15u_xu_{xxxx}+15u_{xx}u_{xxx}+u_{xxxxxx}\right)+\beta\left(6u_xu_{xx}+u_{xxxx}\right)$$
$$+\gamma\left(3\left(u_xu_{xy}+u_{xx}u_y\right)+u_{xxxy}\right)+au_{xx}+bu_{xy}+cu_{xz}-\frac{\gamma^2u_{yy}}{5\alpha}=0, \quad (1)$$

where $u=u(x,y,z,t)$ is a wave function and α,β,γ,a,b and c are arbitrary parameters.
The parameters $\alpha,\beta,\gamma,a,b,andc$ play significant roles in determining the behavior of rogue waves in the pKP-BKP equation that act as a scaling factor for the wave behavior. The parameters are coefficients for the nonlinear terms and dispersion terms of the studied equation, which influence the nonlinearity and dispersion of the rogue wave solution. As these parameters increase, the effect of nonlinearity and dispersion increases, and vice versa. The constants in equation (1) represent the generalized form for the terms where researchers can analyze the solutions for arbitrary choices. Constants a and c are the coefficients of the diffusion terms, so they are called the diffusion coefficients that play an important role in the well-known Burger's equation. The constant b is the coefficient of the disturbed term, so it is called the disturbed coefficient, which has important physical significance in well-known KP-type evolution equations. These constants play a leading role in analyzing the diffusion and disturbance effects for nonlinear models. Therefore, the more coefficients there are, the more opportunities there are to investigate the models with different arbitrary choices. It will provide an understanding of the terms and their coefficients, which facilitates a more comprehensive analysis of nonlinear systems. Together, these parameters dictate the fundamental properties of wave motion, including amplitude, interaction behavior, and localization. Their interplay determines whether the system exhibits stable solitons, rogue waves, or dispersive wave structures. It makes them critical for understanding the underlying wave dynamics in nonlinear systems.
Rogue waves, or extreme waves [12–15] are large amplitude waves that can appear suddenly in the ocean. These waves pose significant risks; they are unpredictable and can cause severe harm, even death. Studying rogue waves is essential for many researchers in nonlinear fields, such as fluid dynamics, optical fiber, and plasma physics. They can be identified by their height, distinguishing them from surrounding waves.

Because rogue waves do not conform to traditional linear wave models, their investigation is crucial for understanding the dynamics of nonlinear waves. This scientific research predicts the occurrence of unusual and massive waves and uncovers their underlying principles to improve maritime safety. Rogue waves can be dangerous, so we need enhancing models and prediction algorithms that can provide early warnings to prevent disasters. This knowledge benefits offshore petroleum and gas operations, coastal communities, and the maritime industry. We understand the development and formation of rogue wave structures for developing adequate safety and mitigation strategies. As a result, we can achieve higher operational security and better explanations of these phenomena. Investigating the dynamics and origins of rogues contributes to understanding the complex processes and nonlinear events that drive these phenomena.
Several fields of nonlinear science and engineering utilize nonlinear PDEs [16–20] to illustrate complex physical processes. Researchers in mathematics have utilized nonlinear PDEs to explain a wide range of scientific phenomena, including fluid dynamics and gravitational studies. The lack of universal methods makes nonlinear PDE analysis and solution difficult. PDEs play a significant role in representing and comprehending physical phenomena involving multiple variables and their rates of change across a wide range of nonlinear sciences. Various techniques obtain exact and analytic solutions for the nonlinear PDEs such as the Hirota's bilinear method [21–23], the Bäcklund transformation [24–26], direct symbolic approach [27,28], the simplified Hirota's approach [29, 30], inverse scattering method [31, 32], symbolic bilinear technique [33], the Darboux transformation [34–38], the Analysis of Lie symmetries [39–42], bilinear neural network techniques [43–45], and other methods such as Wang et al. [46] successfully developed the dressing method and deduced the three-component coupled Hirota hierarchy and gave its soliton solutions.

This article is structured as: The coming section discusses the bilinear form of the studied equation in reduced dimensions using a direct symbolic technique. It reveals the logarithmic transformation applied to new variables and the associated dispersion for the transformed equation. Additionally, it presents the Hirota bilinear form of the transformed equation using Hirota's D-operators. In Section 3, higher-order rogue wave solutions are obtained, including the successful derivation of rogue waves up to the third order. The solutions dynamics are illustrated in both the original and changing variables. Section 4 emphasizes the significant results and findings related to the constructed rogue waves, while the concluding section highlights the importance of this research investigation.

2 Direct symbolic approach and bilinear form

Let us consider a nonlinear partial differential equation (NLPDE) in (3+1)-dimensional variables x, y, z and t as

$$\aleph(u, u_x, u_{xx}, u_y, u_{yy}, u_z, u_{zz}, u_t, u_{xt}, u_{xy}, \cdots) = 0, \tag{2}$$

having partial derivatives with respect to x, y, z and t.
First, we transform the given NLPDE (2) by

$$u = u(\xi, \eta), \qquad \xi = c_1 x + c_2 t, \quad \eta = c_3 y + c_4 z, \tag{3}$$

where $c_j; 1 \leq j \leq 4$ are real parameters. The transformation (3) reduces the equation (2) into a an equation in (1+1)-dimensional NLPDE as

$$\Im(u, u_\xi, u_{\xi\xi}, u_\eta, u_{\xi\eta}, u_{\eta\eta}, \cdots) = 0. \tag{4}$$

We consider a Cole-Hopf transformation as

$$u = R\{\log g(\xi, \eta)\}_{r\xi}, \tag{5}$$

where R is a constant and g is an auxiliary function. The constant r is the order of ξ, comes from the balance between the highest-order and nonlinear terms in equation (4). The equation (5) transforms the equation (4) into a bilinear form equation in g, by using the Hirota's D-operators [10]

$$D_{\mu}^{n_1} D_{\nu}^{n_2} g(\mu,\nu) g'(\mu,\nu) = \left(\frac{\partial}{\partial_{\mu}} - \frac{\partial}{\partial_{\mu'}}\right)^{n_1} \left(\frac{\partial}{\partial_{\nu}} - \frac{\partial}{\partial_{\nu'}}\right)^{n_2} g(\mu,\nu) g'(\mu',\nu')|_{\mu=\mu',\nu=\nu',g=g'},$$

having μ', ν' are formal variables and $n_{i=1,2}$ are non-negative integers.
To obtain the n-rogue waves, we take a generalized form for auxiliary function g designed by Kumar and Mohan [47] as

$$g(\xi,\eta) = \sum_{p=0}^{\frac{q}{2}(q+1)} \sum_{j=0}^{p} c_{q(q+1)-2p,2j} (\xi)^{q(q+1)-2p} (\eta)^{2j}, \tag{6}$$

where $c_{m,n}; m, n \in \{0, 2, \cdots, p(p+1)\}$ are the constants.
Theorem 1: Under the transformations $\xi = x + t$ and $\eta = y + z$, the equation (1) reduces to a (1+1)-dimensional equation and gives a Hirota bilinear form as

$$\left[\alpha D_{\xi}^6 + \beta D_{\xi}^4 + \gamma D_{\xi}^3 D_{\eta} + (1+a) D_{\xi}^2 + (b+c) D_{\xi} D_{\eta} - \frac{\gamma^2}{5\alpha} D_{\eta}^2\right] f.f = 0.$$

Proof: We consider the transformation $u(x, y, z, t) = u(\xi, \eta)$ with $\xi = x + t$ and $\eta = y + z$ to transform the equation (1) as

$$\alpha(45u_{\xi}^2 u_{\xi\xi} + 15u_{\xi} u_{\xi\xi\xi\xi} + 15u_{\xi\xi} u_{\xi\xi\xi} + u_{\xi\xi\xi\xi\xi\xi}) + \beta(6u_{\xi} u_{\xi\xi} + u_{\xi\xi\xi\xi}) + \gamma(3u_{\eta} u_{\xi\xi} + 3u_{\xi} u_{\xi\eta} + u_{\xi\xi\xi\eta}) + (1+a) u_{\xi\xi} + (b+c) u_{\xi\eta} - \frac{\gamma^2 u_{\eta\eta}}{5\alpha} = 0. \tag{7}$$

Let the phase for the equation (7) is

$$\theta_i = p_i \xi - w_i \eta, \tag{8}$$

where $p_{i\in N}$ and $w_{i\in N}$ are constant parameters and dispersion, respectively. We get the dispesion value by substituting $u(\xi, \eta) = e^{\theta_i}$ in linear terms of Eq. (7) as

$$w_i = \frac{-5\alpha(bp_i + cp_i + \gamma p_i^3) \pm \sqrt{4\alpha\gamma^2 p_i^2 \left(5a + 5\alpha p_i^4 + 5\beta p_i^2 + 5\right) + \alpha^2 p_i^2 \left(5b + 5c + 5\gamma p_i^2\right)^2}}{2\gamma^2}. \tag{9}$$

Taking the Cole-Hopf logarithmic transformation

$$u(\xi,\eta) = Q(\log f)_{\xi}, \tag{10}$$

with auxiliary function $f(\xi, \eta)$, and finds the constant $Q = 2$ by putting equation (10) in the equation (7) having $f = 1 + e^{\theta_1}$. Now, on substituting the equation (10) into transformed equation (7), we get a bilinear equation in f as

$$\alpha(f f_{\xi\xi\xi\xi\xi\xi} - 6f_{\xi} f_{\xi\xi\xi\xi\xi} + 15 f_{\xi\xi\xi\xi} f_{\xi\xi} - 10 f_{\xi\xi\xi}^2) + \beta(f f_{\xi\xi\xi\xi} - 4 f_{\xi\xi\xi} f_{\xi} + 3 f_{\xi\xi}^2) + \gamma(f f_{\xi\xi\xi\eta} - 3 f_{\xi} f_{\xi\xi\eta} + 3 f_{\xi\xi} f_{\xi\eta} - f_{\xi\xi\xi} f_{\eta}) + (1+a)(f f_{\xi\xi} - f_{\xi}^2) + (b+c)(f f_{\xi\eta} - f_{\xi\eta}) - \frac{\gamma^2}{5\alpha}(f f_{\eta\eta} - f_{\eta}^2) = 0, \tag{11}$$

which writes in the Hirota's bilinear form as

$$\left[\alpha D_{\xi}^6 + \beta D_{\xi}^4 + \gamma D_{\xi}^3 D_{\eta} + (1+a) D_{\xi}^2 + (b+c) D_{\xi} D_{\eta} - \frac{\gamma^2}{5\alpha} D_{\eta}^2\right] f.f = 0. \tag{12}$$

3 Higher-order rogue waves

Theorem 2: The higher-order rogue waves for a (1+1)-dimensional transformed equation (12), are

$$f(\xi,\eta)=\sum_{q=0}^{\frac{n(n+1)}{2}}\sum_{i=0}^{q}s_{n(n+1)-2q,2i}\xi^{n(n+1)-2q}\eta^{2i},$$

where $s_{j,k}$ are real parameters with $j,k=0,2,\cdots,q(q+1)$.

Proof: To obtain the solutions for rogue waves, we consider the auxiliary function f as given in the generalized form (6). With the inductive analysis of the generalized rogue wave solutions, we consider the different values of n from one to three to show the obtained rogue waves up to the third-order. It illustrates the solutions for different n in the expressed auxiliary function f. We compute the unknown constants $s_{j,k}$ where j and k have the restricted notation as $j,k=0,2,4,...,q(q+1)$ where $0\leq q\leq\frac{n(n+1)}{2}$, to get the correct expression of constant corresponding to the terms. As we go for the higher values of n, the number of constants increases rapidly. For $n=1$, $n=2$, and $n=3$, we have 3, 10, and 28 constants, those we have to find out for a valid solution. These parameters are arbitrary as dependent on the one arbitrary parameter for each case, as in constant values (10), the arbitrary parameter is $s_{2,0}$, and similarly for the next cases for n=2 and 3.

3.1 First-order wave solutions

We take the function f with $n=1$ in equation (3) as

$$f(\xi,\eta)=f_1=s_{0,0}+s_{0,2}\eta^2+s_{2,0}\xi^2. \tag{13}$$

Substituting the equation (13) into (11), and equating the coefficients for different exponents in ξ and η to zero gives a system as

$$\begin{aligned}30\alpha\beta s_{2,0}^2-s_{0,0}\left(\gamma^2 s_{0,2}-5(a+1)\alpha s_{2,0}\right)&=0,\\ s_{2,0}\left(-5(a+1)\alpha s_{2,0}-\gamma^2 s_{0,2}\right)&=0,\\ s_{0,2}\left(5(a+1)\alpha s_{2,0}+\gamma^2 s_{0,2}\right)&=0.\end{aligned} \tag{14}$$

On solving the system, we get

$$s_{0,0}=-\frac{3\beta s_{2,0}}{a+1},\qquad s_{0,2}=-\frac{5(a+1)\alpha s_{2,0}}{\gamma^2},\qquad s_{2,0}=s_{2,0}. \tag{15}$$

Thus, the function (13) becomes

$$f=\left(-\frac{5(a+1)\alpha\eta^2}{\gamma^2}-\frac{3\beta}{a+1}+\xi^2\right)s_{2,0}, \tag{16}$$

that gives first-order rogue solutions by substituting the equation (16) into (10) as

$$u=\frac{4\xi}{-\frac{5(a+1)\alpha\eta^2}{\gamma^2}-\frac{3\beta}{a+1}+\xi^2}, \tag{17}$$

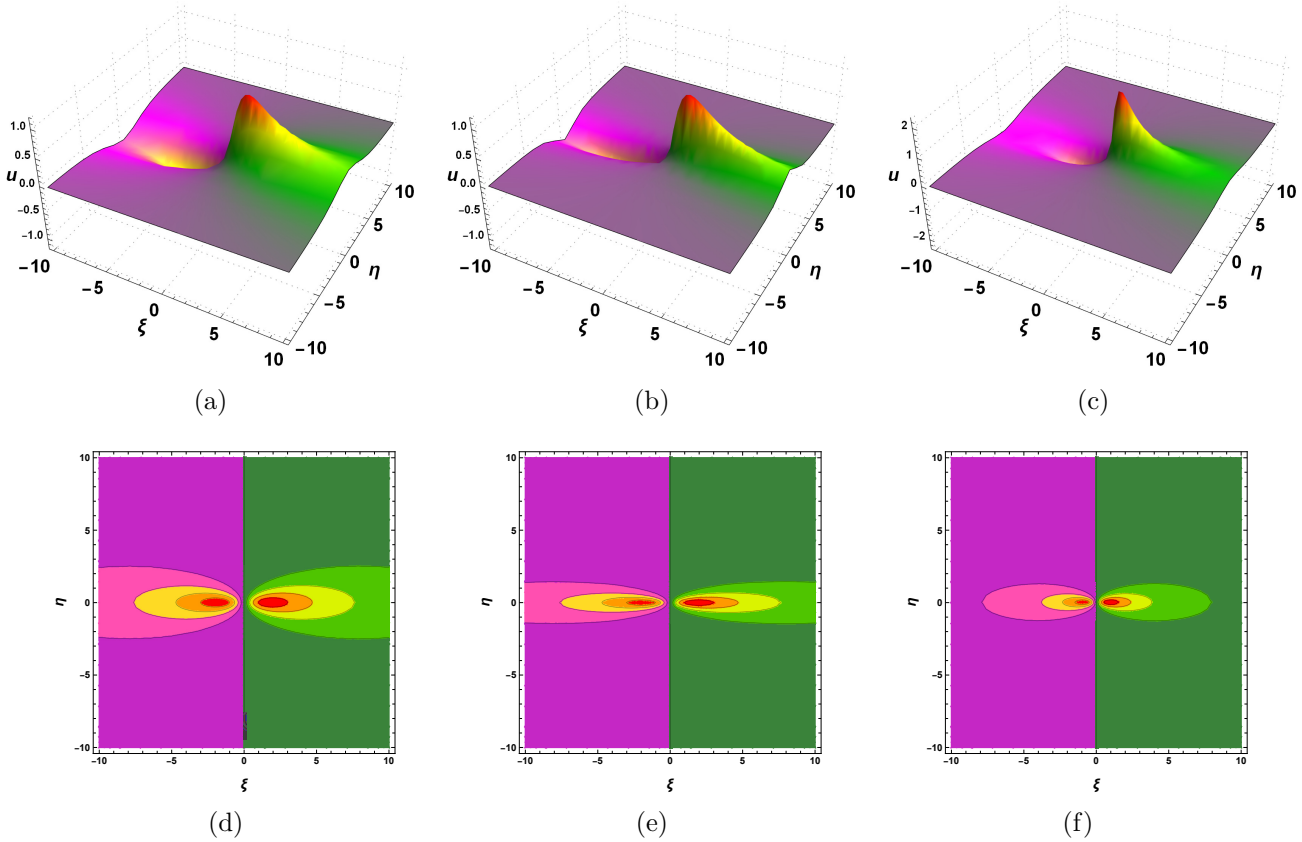

Figure 1: Dynamical profiles for the solution (17), and figures **(d)-(f)** depicts contour plots for **(a)-(c)**.

3.2 Second-order wave solutions

Having $n = 2$ in equation (3) the function f becomes

$$f(\xi,\eta) = f_2 = s_{0,0} + s_{0,2}\eta^2 + s_{0,4}\eta^4 + s_{0,6}\eta^6 + s_{2,0}\xi^2 + s_{2,2}\eta^2\xi^2 + s_{2,4}\eta^4\xi^2 + s_{4,0}\xi^4 + s_{4,2}\eta^2\xi^4 + s_{6,0}\xi^6. \quad (18)$$

Substituting the equation (18) into (12) and equating the coefficients for different exponents in ξ and η to zero gives a system and retrieves the values as

$$s_{0,0} = \frac{5\gamma^2\left(4(a+1)^2\alpha^2 - 80(a+1)\alpha\beta^2 + 25\beta^4\right)s_{4,2}}{(a+1)^4\alpha\beta}, \quad s_{0,2} = \frac{5\left(20(a+1)^2\alpha^2 - 124(a+1)\alpha\beta^2 + 95\beta^4\right)s_{4,2}}{3(a+1)^2\beta^2},$$

$$s_{0,4} = -\frac{5\alpha\left(20(a+1)\alpha - 17\beta^2\right)s_{4,2}}{3\beta\gamma^2}, \quad s_{0,6} = \frac{25(a+1)^2\alpha^2 s_{4,2}}{3\gamma^4},$$

$$s_{2,0} = -\frac{5\gamma^2\left(4(a+1)^2\alpha^2 + 28(a+1)\alpha\beta^2 - 5\beta^4\right)s_{4,2}}{3(a+1)^3\alpha\beta^2}, \quad s_{2,2} = -\frac{30\beta s_{4,2}}{a+1},$$

$$s_{2,4} = -\frac{5(a\alpha+\alpha)s_{4,2}}{\gamma^2}, \quad s_{4,0} = \frac{\gamma^2\left(4a\alpha + 4\alpha + 5\beta^2\right)s_{4,2}}{3(a+1)^2\alpha\beta}, \quad s_{4,2} = s_{4,2},$$

$$s_{6,0} = -\frac{\gamma^2 s_{4,2}}{15(a+1)\alpha}, \quad (19)$$

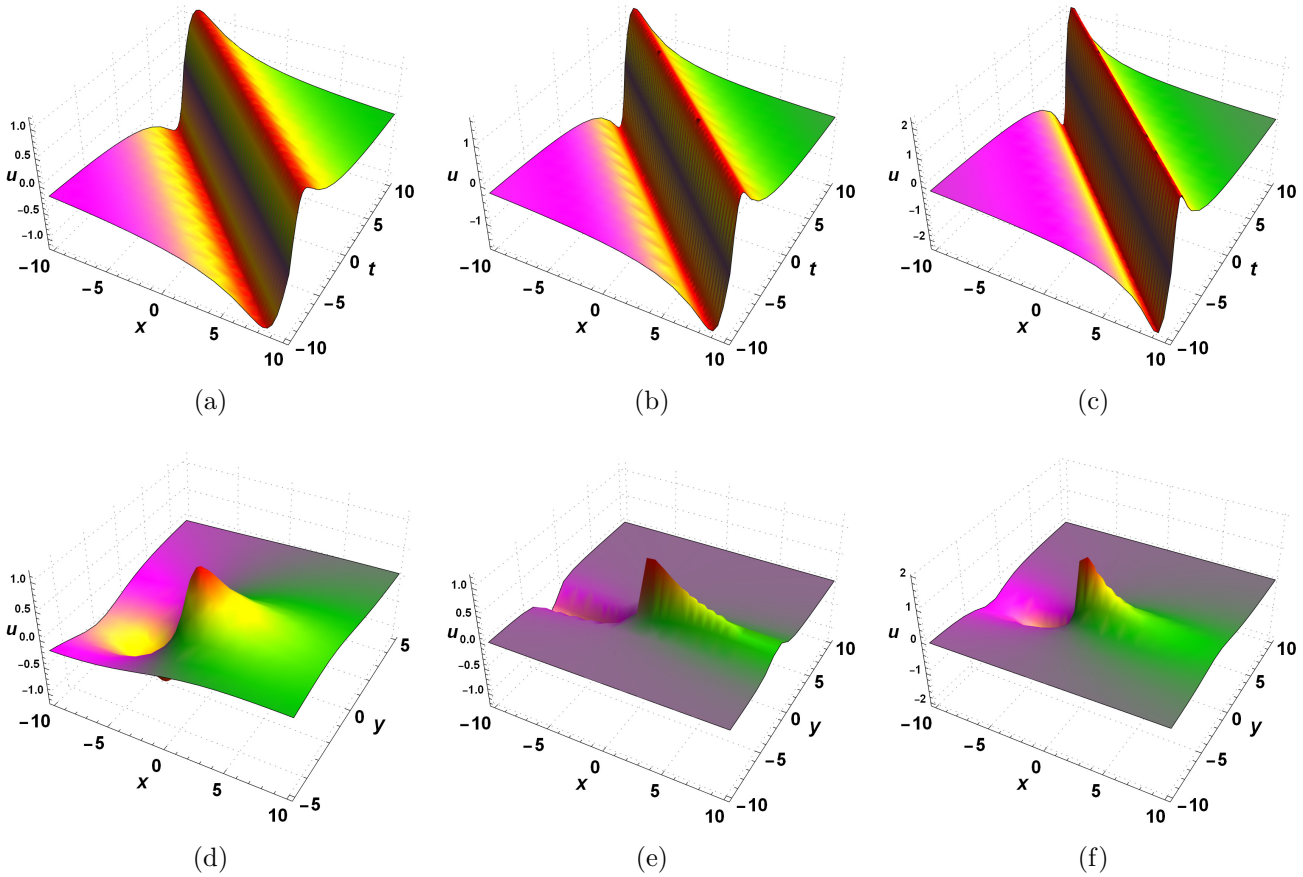

Figure 2: Dynamics of solution (17) in original variables $\{x, y, z, t\}$, and figures **(a-c)** and **(d-f)** show wave dynamics in xt-planes and xy-planes.

Therefore, the function (13) becomes

$$f(\xi,\eta) = \frac{s_{4,2}}{15}\Big(-\frac{25\gamma^2\xi^2\left(4(a+1)^2\alpha^2+28(a+1)\alpha\beta^2-5\beta^4\right)}{(a+1)^3\alpha\beta^2} + \frac{75\gamma^2\left(4(a+1)^2\alpha^2-80(a+1)\alpha\beta^2+25\beta^4\right)}{(a+1)^4\alpha\beta} + \frac{25\eta^2\left(20(a+1)^2\alpha^2-124(a+1)\alpha\beta^2+95\beta^4\right)}{(a+1)^2\beta^2} + \frac{125(a+1)^2\alpha^2\eta^6}{\gamma^4} - \frac{25\alpha\eta^4\left(20(a+1)\alpha-17\beta^2\right)}{\beta\gamma^2} + \frac{5\gamma^2\xi^4\left(4(a+1)\alpha+5\beta^2\right)}{(a+1)^2\alpha\beta} - \frac{75(a+1)\alpha\eta^4\xi^2}{\gamma^2} - \frac{\gamma^2\xi^6}{a\alpha+\alpha} - \frac{450\beta\eta^2\xi^2}{a+1} + 15\eta^2\xi^4\Big), \quad (20)$$

Thus, we obtain the second-order solution by substituting the Eq. (20) into (10)

$$u(\xi,\eta) = 2(\log f_2)_\xi. \quad (21)$$

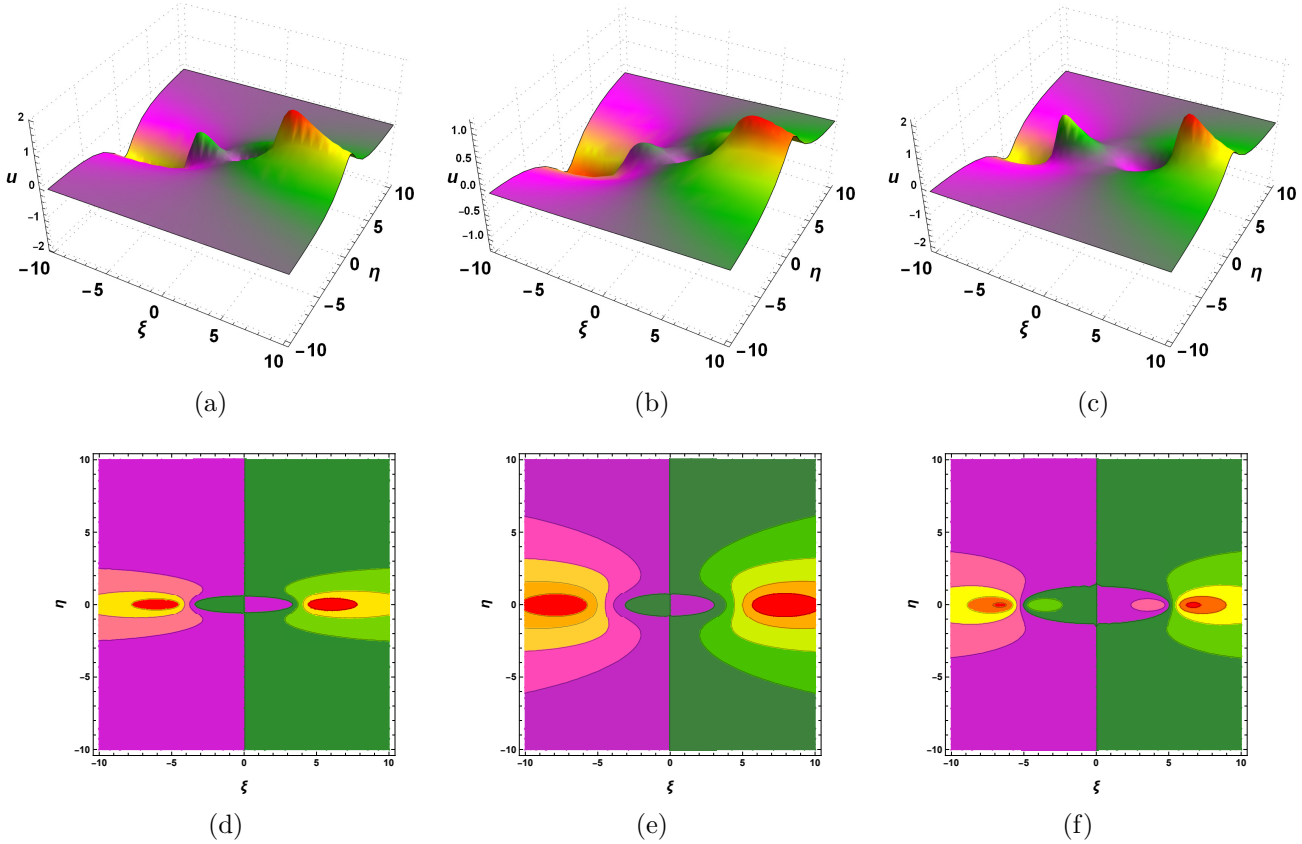

Figure 3: Dynamical profiles for the solution (21), and figures **(d)-(f)** depicts contour plots for **(a)-(c)**.

3.3 Third-order rogue waves

Having $n = 3$ in equation (3) gives third-order rogue waves with function f as

$$f(\xi,\eta) = f_3 = s_{0,0} + s_{0,2}\eta^2 + s_{0,4}\eta^4 + s_{0,6}\eta^6 + s_{0,8}\eta^8 + s_{0,10}\eta^{10} + s_{0,12}\eta^{12} + s_{2,0}\xi^2 + s_{2,2}\xi^2\eta^2 + s_{2,4}\xi^2\eta^4 + s_{2,6}\xi^2\eta^6 + s_{2,8}\xi^2\eta^8 + s_{2,10}\xi^2\eta^{10} + s_{4,0}\xi^4 + s_{4,2}\xi^4\eta^2 + s_{4,4}\xi^4\eta^4 + s_{4,6}\xi^4\eta^6 + s_{4,8}\xi^4\eta^8 + s_{6,0}\xi^6 + s_{6,2}\xi^6\eta^2 + s_{6,4}\xi^6\eta^4 + s_{6,6}\xi^6\eta^6 + s_{8,0}\xi^8 + s_{8,2}\xi^8\eta^2 + s_{8,4}\xi^8\eta^4 + s_{10,0}\xi^{10} + s_{10,2}\xi^{10}\eta^2 + s_{12,0}\xi^{12}. \quad (22)$$

We put the Eq. (18) into Eq. (12), and equating all coefficients for different powers in ξ and η to zero gives a set of equations that gives the constants on solving as

$$s_{0,0} = -\frac{\gamma^2 s_{10,2}}{2646(a+1)^7\alpha\beta^6}(885912165012(a+1)^2\alpha^2\beta^8 - 783353946256(a+1)^3\alpha^3\beta^6 - 2059366141680(a+1)^4\alpha^4\beta^4 + 356841168000(a+1)^5\alpha^5\beta^2 + 18313352000(a+1)^6\alpha^6 - 37581796560(a+1)\alpha\beta^{10} + 8612495045\beta^{12}),$$

$$s_{0,2} = \frac{5s_{10,2}}{63(a+1)^5\beta^5}(-467721272(a+1)^2\alpha^2\beta^6 - 2165184544(a+1)^3\alpha^3\beta^4 + 637800080(a+1)^4\alpha^4\beta^2 + 30260000(a+1)^5\alpha^5 + 969547810(a+1)\alpha\beta^8 - 210627725\beta^{10}),$$

$$s_{0,4} = \frac{125\alpha s_{10,2}}{126(a+1)^3\beta^4\gamma^2}(2016624(a+1)^2\alpha^2\beta^4 - 33319520(a+1)^3\alpha^3\beta^2 + 1000400(a+1)^4\alpha^4 + 19367152(a+1)\alpha\beta^6 - 4589683\beta^8),$$

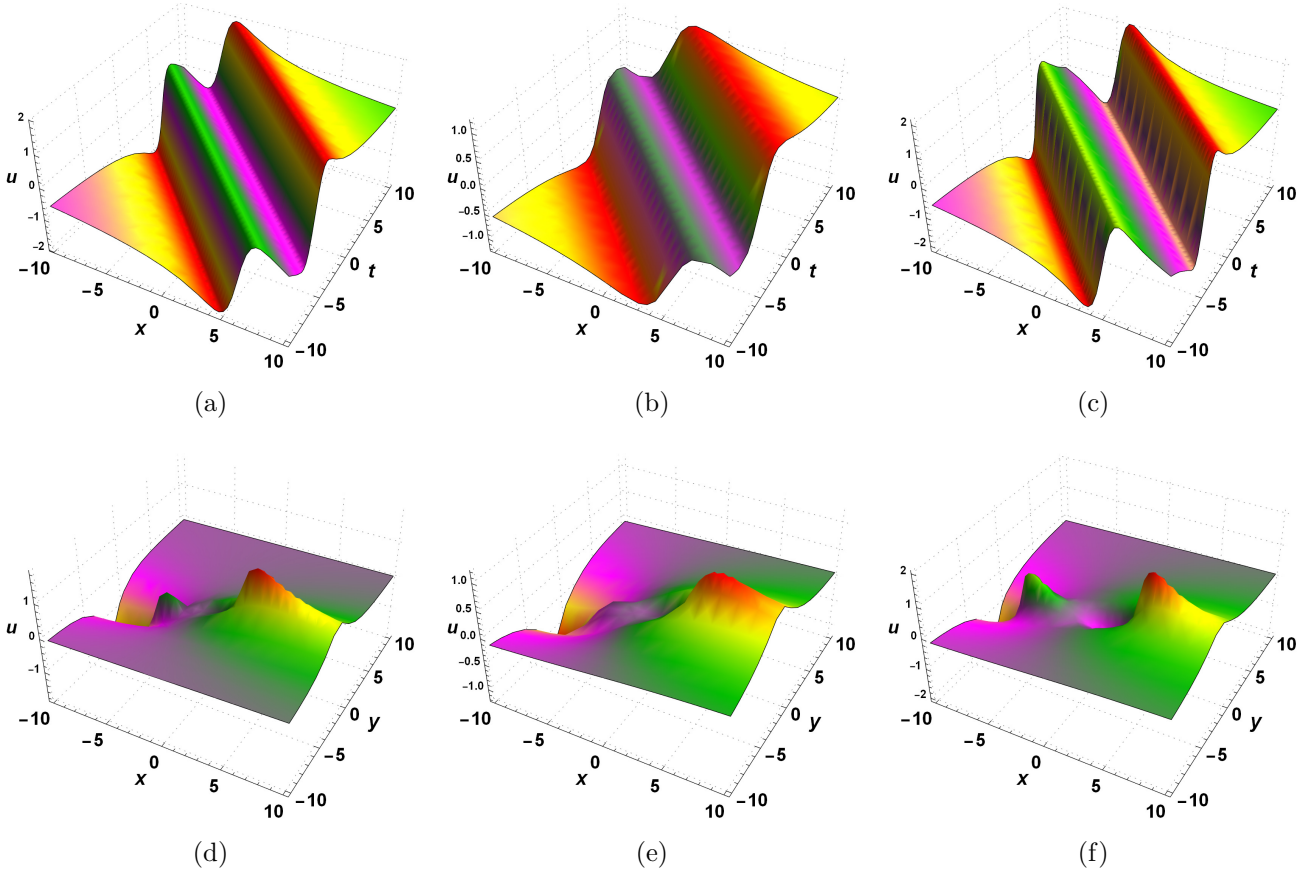

Figure 4: Dynamics of solution (21) in original variables $\{x, y, z, t\}$, and figures **(a-c)** and **(d-f)** show wave profiles in xt-planes and xy-planes.

$$s_{0,6} = -\frac{250\alpha^2 s_{10,2}}{63(a+1)\beta^3\gamma^4}\left(221880(a+1)^2\alpha^2\beta^2 + 82760(a+1)^3\alpha^3 - 714126(a+1)\alpha\beta^4 + 279643\beta^6\right),$$

$$s_{0,8} = -\frac{625(a+1)\alpha^3\left(100(a+1)^2\alpha^2 - 608(a+1)\alpha\beta^2 + 289\beta^4\right)s_{10,2}}{2\beta^2\gamma^6},$$

$$s_{0,10} = \frac{625(a+1)^3\alpha^4\left(50(a+1)\alpha - 29\beta^2\right)s_{10,2}}{3\beta\gamma^8}, \qquad s_{0,12} = -\frac{3125(a+1)^5\alpha^5 s_{10,2}}{6\gamma^{10}},$$

$$s_{2,0} = \frac{\gamma^2 s_{10,2}}{63(a+1)^6\alpha\beta^5}(601571032(a+1)^2\alpha^2\beta^6 - 12245056(a+1)^3\alpha^3\beta^4 + 51769520(a+1)^4\alpha^4\beta^2$$
$$+30260000(a+1)^5\alpha^5 - 624620150(a+1)\alpha\beta^8 + 111850585\beta^{10}),$$

$$s_{2,4} = -\frac{250\alpha\left(-37480(a+1)^2\alpha^2\beta^2 + 8920(a+1)^3\alpha^3 - 8134(a+1)\alpha\beta^4 + 343\beta^6\right)s_{10,2}}{7(a+1)^2\beta^3\gamma^2},$$

$$s_{2,6} = \frac{250\alpha^2\left(700(a+1)^2\alpha^2 - 1436(a+1)\alpha\beta^2 + 1771\beta^4\right)s_{10,2}}{3\beta^2\gamma^4},$$

$$s_{2,8} = -\frac{625(a+1)^2\alpha^3\left(10(a+1)\alpha - 19\beta^2\right)s_{10,2}}{\beta\gamma^6}, \qquad s_{2,10} = \frac{625(a+1)^4\alpha^4 s_{10,2}}{\gamma^8},$$

$$s_{4,0} = \frac{5\gamma^2 s_{10,2}}{126(a+1)^5\alpha\beta^4}(3719280(a+1)^2\alpha^2\beta^4 - 1436960(a+1)^3\alpha^3\beta^2 + 1000400(a+1)^4\alpha^4$$
$$-6761216(a+1)\alpha\beta^6 + 1452605\beta^8),$$
$$s_{4,2} = -\frac{50\left(25240(a+1)^2\alpha^2\beta^2 + 8920(a+1)^3\alpha^3 + 11662(a+1)\alpha\beta^4 + 5145\beta^6\right)s_{10,2}}{7(a+1)^3\beta^3},$$
$$s_{4,4} = -\frac{125\alpha\left(500(a+1)^2\alpha^2 + 56(a+1)\alpha\beta^2 + 749\beta^4\right)s_{10,2}}{3(a+1)\beta^2\gamma^2},$$
$$s_{4,6} = \frac{250(a+1)\alpha^2\left(10(a+1)\alpha - 73\beta^2\right)s_{10,2}}{3\beta\gamma^4}, \quad s_{4,8} = -\frac{625(a+1)^3\alpha^3 s_{10,2}}{2\gamma^6},$$
$$s_{6,0} = -\frac{2\gamma^2\left(-272040(a+1)^2\alpha^2\beta^2 + 82760(a+1)^3\alpha^3 + 14406(a+1)\alpha\beta^4 - 26411\beta^6\right)s_{10,2}}{63(a+1)^4\alpha\beta^3},$$
$$s_{6,2} = \frac{70\left(100(a+1)^2\alpha^2 + 244(a+1)\alpha\beta^2 + 133\beta^4\right)s_{10,2}}{3(a+1)^2\beta^2}, \quad s_{6,4} = \frac{50\alpha\left(10(a+1)\alpha + 77\beta^2\right)s_{10,2}}{3\beta\gamma^2},$$
$$s_{6,6} = \frac{250(a+1)^2\alpha^2 s_{10,2}}{3\gamma^4}, \quad s_{8,0} = -\frac{\gamma^2\left(100(a+1)^2\alpha^2 + 784(a+1)\alpha\beta^2 + 49\beta^4\right)s_{10,2}}{2(a+1)^3\alpha\beta^2},$$
$$s_{8,2} = -\frac{5\left(10(a+1)\alpha + 23\beta^2\right)s_{10,2}}{(a+1)\beta}, \quad s_{8,4} = -\frac{25(a\alpha+\alpha)s_{10,2}}{2\gamma^2}, \quad s_{10,0} = \frac{\gamma^2\left(50(a+1)\alpha + 49\beta^2\right)s_{10,2}}{15(a+1)^2\alpha\beta},$$
$$s_{10,2} = s_{10,2}, \quad s_{12,0} = -\frac{\gamma^2 s_{10,2}}{30(a+1)\alpha}. \tag{23}$$

Thus, we obtain the solution for third order by having the Eq. (22) with values (23) into (10)

$$u(\xi,\eta) = 2(\log f_3)_\xi. \tag{24}$$

4 Results and findings

By applying the appropriate parameter values, the equation under investigation demonstrated rogue wave shapes in the transformed variables ξ and η. A bilinear symbolic technique was employed to solve the studied pKP-BKP equation for higher-order rogue waves. The first-order rogue wave solution produced a single rogue wave, while the second and third-order solutions resulted in two and three rogue wave interactions, respectively. We illustrated the dynamics of these rogue waves for the obtained solutions in both the transformed variables $\{\xi,\eta\}$ and the original variables $\{x,y,z,t\}$. The dynamical profiles explore the representation of the waves in the planes defined by $\{\xi,\eta\}$, $\{x,t\}$, and $\{x,y\}$. The dynamics observed in the xt-plane reveal the interactions among the rogue waves in either the $\xi\eta$ or xy-planes. The findings of this study can be summarized as follows:

- In Figure-1 and Figure-2, we illustrate the rogue waves of 1^{st}-order , which depict the single rogue waves with singularities at $\xi = 0$ and $\eta = 0$. Rogue waves in Figure-1 display the bright parts in the positive direction of ξ and the dark parts in the negative direction of ξ. Figure-2 depicts the single rogue structures with the initial variables x, y, z, t of the studied equation. Graphics $(a-c)$ illustrate the single waves concerning xt-planes having $y = 0$ and $z = 0$, and graphics $(d-f)$ depicts the single rogue waves in xy-planes having $z = 2$ and $t = 2$. The graphics were generated with the values of parameters as **(a), (d)** $\alpha = -1, \beta = -2, \gamma = a = 1$; **(b), (e)** $\alpha = -2, \beta = -3, \gamma = 1, a = 2$; and **(c), (f)** $\alpha = -1, \beta = -0.5, \gamma = -1, a = 1$.

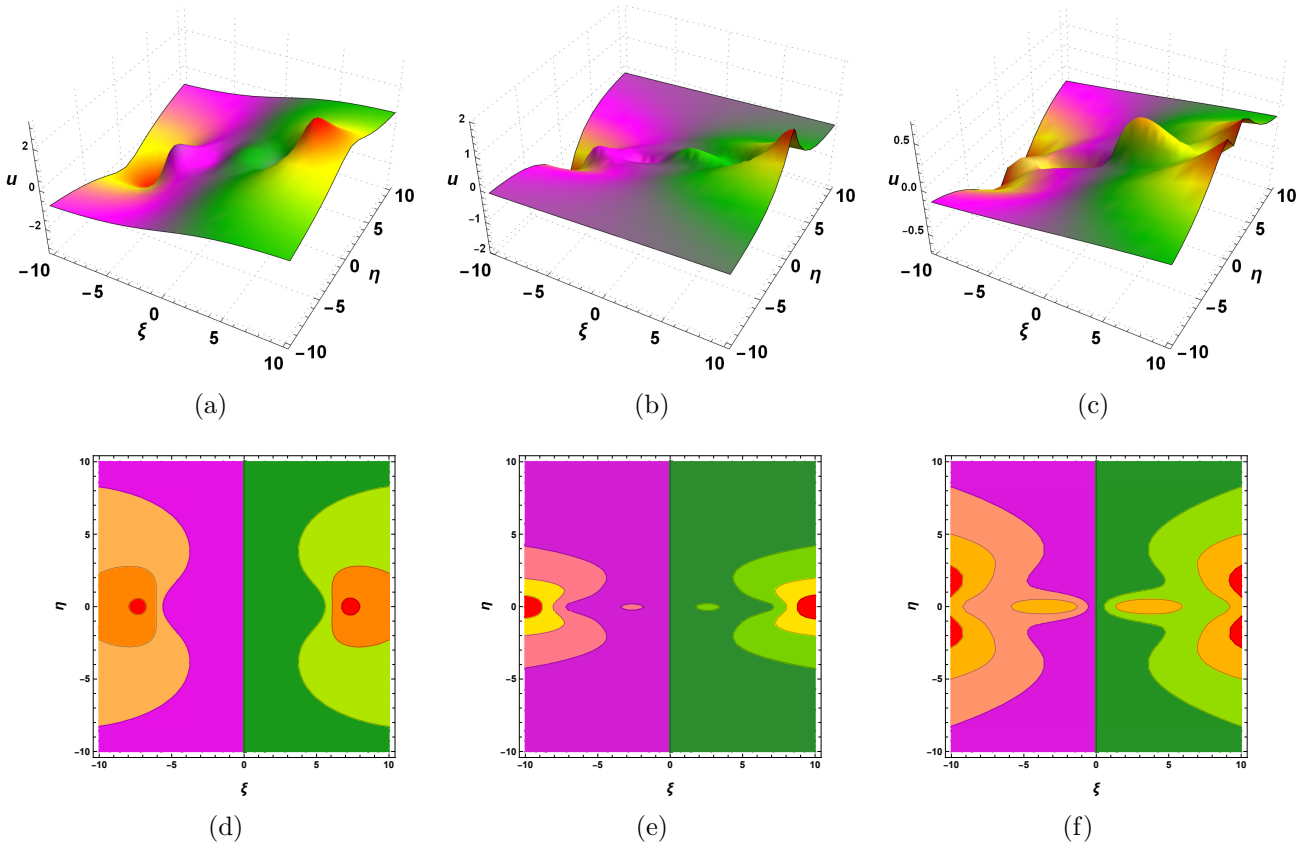

Figure 5: Dynamical profiles for the third-order rogue waves with solution (24) in ξ and η. The figures **(d)-(f)** depicts contour plots for **(a)-(c)**.

- Figure-3 and Figure-4 depict rogue waves of 2^{nd}-order showing two rogue-wave interactions. Rogue waves in Figure-3 intersect at $\xi = 0$ and $\eta = 0$ displaying the bright-dark parts. Figure-4 displays two rogue waves in x, y, z, t, the initial variables of the studied equation. Graphics $(a-c)$ depict two waves in xt-plane with $y = 0$ and $z = 0$, and graphics $(d-f)$ depict the two rogue waves in xy-plane with $z = 2$ and $t = 2$. The figures were developed with the values of parameters as **(a), (d)** $\alpha = -2, \beta = -3, \gamma = a = 1$; **(b), (e)** $\alpha = -1, \beta = -7, \gamma = a = 1$; and **(c), (f)** $\alpha = -7, \beta = -4, \gamma = 3, a = 1$.

- In Figure-5 and Figure-6, we illustrate the rogue waves of 3^{rd}-order depicting three rogue-wave interactions. Rogue waves in Figure-5 depict two interactions of three rogue waves with their bight-dark parts. In Figure-6, we show the three waves in x, y, z, t, the initial variables in the investigated equation. Graphics $(a-c)$ depict three waves in xt-plane with $y = 0$ and $z = 0$, and graphics $(d-f)$ shows the interaction of three rogue waves in xy-plane with $z = 2$ and $t = 2$. The graphics were generated with the values of parameters as **(a), (d)** $\alpha = -1, \beta = -3, \gamma = 3, a = 2$; **(b), (e)** $\alpha = -2, \beta = -5, \gamma = 1, a = 1$; and **(c), (f)** $\alpha = -2, \beta = -10, \gamma = 1, a = 0.7$.

5 Conclusions

This research successfully explored the higher-order rogue waves of the (3+1)-dimensional pKP-BKP equation within fluid dynamics. By employing a bilinear symbolic approach, we generated rogue waves up to the third order with a generalized formula having real parameters. It established Hirota's D-operator bilinear

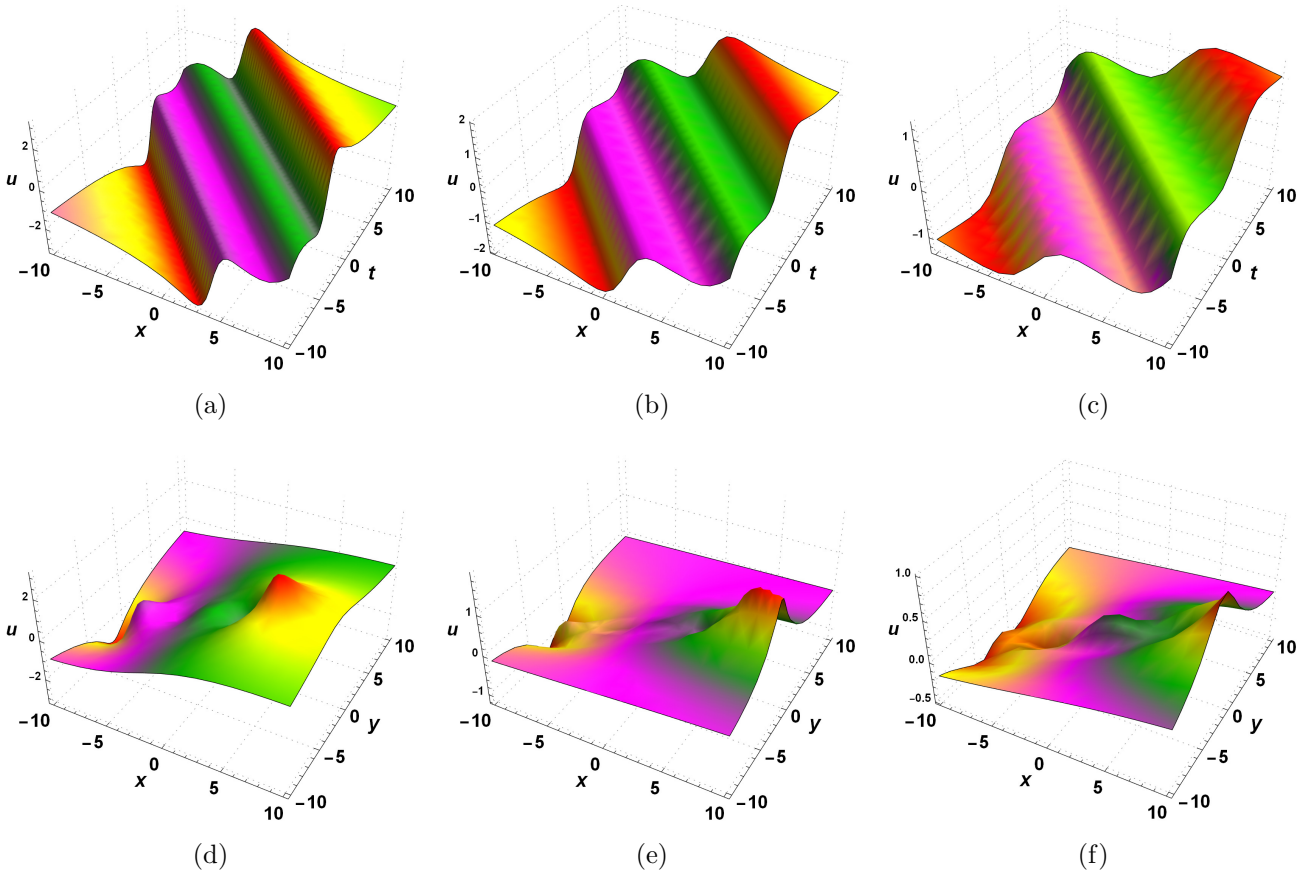

Figure 6: Dynamics of solution (24) in original variables x, y, z, and t with transformations $\{\xi = x + t, \eta = y + z\}$. The figures **(a-c)** and **(d-f)** show wave profiles in xt- and xy-planes.

form for the equation in transformed variables. It demonstrated that 2^{nd}- and 3^{rd}-order rogue wave solutions result in two and three rogue interactions, respectively. Our findings illustrated that these significant rogue waves interact locally within nonlinear processes, a critical insight for understanding their behavior. We derived a bilinear equation by utilizing the logarithmic transformation and facilitating a dynamic analysis of the obtained solutions. Symbolic system *Mathematica* enabled the visualization of these solutions in ξ, η and x, y, z, t, the transformed and initial variables, respectively.

The study highlights the evolution of smaller-amplitude rogue waves, which are particularly significant in plasma physics, fluid dynamics, and nonlinear systems. The findings offer valuable insights into these phenomena' mechanisms and contribute significantly to various scientific fields such as oceanography, plasma physics, dusty plasma, water engineering, optical fibers, and nonlinear systems. This research enhances our understanding of rogue waves and their interactions and broadens the knowledge base in these important areas of study.

Declarations

Ethics approval and consent to participate

Not applicable.

Conflict of interest

The author claims that there are no conflicts of interest.

Data availability statement

No datasets have been generated or analyzed during the current investigation.

References

[1] Ren, B., Yu, J., Liu, X.Z.: Nonlocal Symmetries and Interaction Solutions for Potential Kadomtsev–Petviashvili Equation, Commun. Theor. Phys. **65**(3), 341 (2016)

[2] Abazari, R.: A modified form of $\frac{G'}{G}$-expansion method and its application to Potential Kadomtsev–Petviashvili (PKP) equation, Japan J. Indust. Appl. Math. 31, 125–136 (2014)

[3] Singh, S., Ray, S.S.: The Painlevé integrability and abundant analytical solutions for the potential Kadomtsev–Petviashvili (pKP) type coupled system with variable coefficients arising in nonlinear physics, Chaos, Solitons Fractals, **175**(1), 113947 (2023)

[4] Du, X. X., Tian, B., Yin, Y.: Lump, mixed lump-kink, breather and rogue waves for a B-type Kadomtsev-Petviashvili equation. Waves in Random and Complex Media, **31**(1), 101–116 (2021)

[5] Yan, X. W., Tian, S. F., Wang, X. B., Zhang, T. T.: Solitons to rogue waves transition, lump solutions and interaction solutions for the (3+1)-dimensional generalized B-type Kadomtsev–Petviashvili equation in fluid dynamics. International Journal of Computer Mathematics, **96**(9), 1839–1848 (2019)

[6] Zhang, H.: A note on exact complex travelling wave solutions for (2+1)-dimensional B-type Kadomtsev–Petviashvili equation, Applied Mathematics and Computation, **216**(9), 2771-2777 (2010)

[7] Ma, W.X.: Lump solutions to the Kadomtsev–Petviashvili equation, Physics Letters A, **379**(36), 1975-1978 (2015)

[8] Wazwaz, AM., El-Tantawy, S.A. A new (3+1)-dimensional generalized Kadomtsev–Petviashvili equation. Nonlinear Dyn **84**, 1107–1112 (2016)

[9] Johnson, R.S.: Water waves and Korteweg–de Vries equations. Journal of Fluid Mechanics, **97**(4), 701-719 (1980)

[10] Hirota R.: The direct method in soliton theory. Cambridge: Cambridge University Press, (2004)

[11] Wazwaz, A.M.: Breather wave solutions for an integrable (3+1)-dimensional combined pKP–BKP equation, Chaos, Solitons Fractals, **182**, 114886 (2024)

[12] Kumar, S., Mohan, B.: A novel analysis of Cole-Hopf transformations in different dimensions, solitons, and rogue waves for a (2+1)-dimensional shallow water wave equation of ion-acoustic waves in plasmas, Physics of Fluids, **35**, 127128, (2023)

[13] Zhang, R.F., Li, M.C., Gan, J.Y., et al.: Novel trial functions and rogue waves of generalized breaking soliton equation via bilinear neural network method, Chaos, Solitons & Fractals, **154**, 111692, (2022)

[14] Mohan, B., Kumar, S., Kumar, R.: Higher-order rogue waves and dispersive solitons of a novel P-type (3+1)-D evolution equation in soliton theory and nonlinear waves, Nonlinear Dynamics, **111**, 20275–20288, (2023)

[15] Li L., Xie Y.: Rogue wave solutions of the generalized (3+1)-dimensional Kadomtsev–Petviashvili equation. Chaos Soli Fract, **147**, 110935, (2021)

[16] Lan, ZZ.: Multi-soliton solutions, breather-like and bound-state solitons for complex modified Korteweg–de Vries equation in optical fibers, Chinese Phys. B, **33** 060201, (2024)

[17] Lan, ZZ.: Multiple Soliton Asymptotics in a Spin-1 Bose–Einstein Condensate, Chinese Phys. Lett., **41**, 090501, (2024)

[18] Zhao, XH.: Multi-solitons and integrability for a (2+1)-dimensional variable coefficients Date–Jimbo–Kashiwara–Miwa equation, Applied Mathematics Letters, **149**, 108895, (2024)

[19] Lan, ZZ.: Semirational rogue waves of the three coupled higher-order nonlinear Schrödinger equations, Applied Mathematics Letters, **147**, 108845, (2024)

[20] Lan, ZZ.: Bound-state solitons in three-wave resonant interactions. Nonlinear Dyn. **112**, 20173–20181 (2024)

[21] Wang, S.: Novel soliton solutions of CNLSEs with Hirota bilinear method. J Opt **52**, 1602–1607 (2023)

[22] Guan, X., Liu, W., Zhou, Q., Biswas, A.: Some lump solutions for a generalized (3+1)-dimensional Kadomtsev–Petviashvili equation, Applied Mathematics and Computation, **366**, 124757 (2020)

[23] Wazwaz A.M.: The Hirota's direct method for multiple soliton solutions for three model equations of shallow water waves. Appl. Math. Comput. **201**, 489–503 (2008)

[24] Huang Z.R., Tian B., Zhen H.L. et al.: Bäcklund transformations and soliton solutions for a (3+1)-dimensional B-type Kadomtsev–Petviashvili equation in fluid dynamics. Nonlinear Dyn. **80**, 1–7 (2015)

[25] Yan, X.W., Tian, S.F., Dong, M.J. et al.: Bäcklund transformation, rogue wave solutions and interaction phenomena for a (3+1)(3+1)-dimensional B-type Kadomtsev–Petviashvili–Boussinesq equation. Nonlinear Dyn. **92**, 709–720 (2018)

[26] Lan, ZZ.: N-soliton solutions, Bäcklund transformation and Lax Pair for a generalized variable-coefficient cylindrical Kadomtsev–Petviashvili equation, Applied Mathematics Letters, **158**, 109239, (2024)

[27] Mohan, B., Kumar, S.: Painlevé analysis, restricted bright-dark N-solitons, and N-rogue waves of a (4+1)-dimensional variable-coefficient generalized KP equation in nonlinear sciences, Nonlinear Dynamics, **112**:11373-11382, (2024)

[28] Mohan, B., Kumar, S.: Rogue-wave structures for a generalized (3+1)-dimensional nonlinear wave equation in liquid with gas bubbles, Physica Scripta, **99**:105291, (2024)

[29] Hereman W., Nuseir A.: Symbolic methods to construct exact solutions of nonlinear partial differential equations. Math Comput Simul, **43**, 13–27 (1997)

[30] Kumar, S., Mohan, B. , Kumar, R. : Lump, soliton, and interaction solutions to a generalized two-mode higher-order nonlinear evolution equation in plasma physics, Nonlinear Dyn, **110**, 693–704 (2022)

[31] Kravchenko V.V.: Inverse Scattering Transform Method in Direct and Inverse Sturm-Liouville Problems. Frontiers in Mathematics, Birkhäuser, Cham., (2020)

[32] Zhou, X.: Inverse scattering transform for the time dependent Schrödinger equation with applications to the KPI equation, Commun. Math. Phys. **128**, 551–564 (1990)

[33] Mohan B. Kumar S.: Generalization and analytic exploration of soliton solutions for nonlinear evolution equations via a novel symbolic approach in fluids and nonlinear sciences, Chinese Journal of Physics, 92:10-21, (2024)

[34] Guan X., Liu W., Zhou, Q. et al.: Darboux transformation and analytic solutions for a generalized super-NLS-mKdV equation. Nonlinear Dyn. **98**, 1491–1500 (2019)

[35] Lan, ZZ.: Rogue wave solutions for a higher-order nonlinear Schrödinger equation in an optical fiber, Applied Mathematics Letters **107**, 106382, (2020)

[36] Wang, X., He, J.: Darboux transformation and general soliton solutions for the reverse space–time nonlocal short pulse equation, Physica D: Nonlinear Phenomena, **446**, 133639, (2023)

[37] Wang, X., He, J.: Rogue waves in a reverse space nonlocal nonlinear Schrödinger equation, Physica D: Nonlinear Phenomena, **469**, 134313, (2024)

[38] Wang, X., Wei, J.: Three types of Darboux transformation and general soliton solutions for the space-shifted nonlocal PT symmetric nonlinear Schrödinger equation, Applied Mathematics Letters, **130**, 107998, (2022)

[39] Nonlaopon K., Mann N., Kumar S., Rezaei S., Abdou M.A.: A variety of closed-form solutions, Painlevé analysis, and solitary wave profiles for modified KdV-Zakharov-Kuznetsov equation in (3+1)-dimensions, Results in Physics, **36**, 105394 (2022)

[40] Carminati, J., Vu, K.: Symbolic Computation and Differential Equations: Lie Symmetries, Journal of Symbolic Computation, **29**(1), 95-116, (2000)

[41] Kumar, S., Kumar, D., Kumar, A.: Lie symmetry analysis for obtaining the abundant exact solutions, optimal system and dynamics of solitons for a higher-dimensional Fokas equation, Chaos, Solitons Fractals, **142**, 110507, (2021)

[42] Kumar, S., Niwas, M. Analyzing multi-peak and lump solutions of the variable-coefficient Boiti–Leon–Manna–Pempinelli equation: a comparative study of the Lie classical method and unified method with applications. Nonlinear Dyn **111**, 22457–22475 (2023)

[43] Zhang, R.F., Li, M.C., Fang, T., et al.: Multiple exact solutions for the dimensionally reduced p-gBKP equation via bilinear neural network method, Modern Physics Letters B, **36**(06), 2150590, (2022)

[44] Zhang, RF., Li, MC., Cherraf , A. et al. The interference wave and the bright and dark soliton for two integro-differential equation by using BNNM. Nonlinear Dyn, **111**, 8637–8646, (2023)

[45] Zhang, R.F., Li, M.C. et al: Generalized lump solutions, classical lump solutions and rogue waves of the (2+1)-dimensional Caudrey-Dodd-Gibbon-Kotera-Sawada-like equation, Applied Mathematics and Computation, **403**, 126201 (2021)

[46] Wang ZY., Tian, SF., Cheng, J; The ∂-dressing method and soliton solutions for the three-component coupled Hirota equations. J. Math. Phys. 1 **62**(9), 093510, (2021)

[47] Kumar, S., Mohan, B.: A direct symbolic computation of center-controlled rogue waves to a new Painlevé-integrable (3+1)-D generalized nonlinear evolution equation in plasmas. Nonlinear Dyn, **111**, 16395–16405, (2023)